UCRL-JC-111464
PREPRINT

# Correlation of Damage Threshold and Surface Geometry of Nodular Defects in HR Coatings As Determined by In-Situ Atomic Force Microscopy

M.C. Staggs, M.R. Kozlowski, W. J. Siekhaus and M. Balooch
Lawrence Livermore National Laboratory

This paper was prepared for submittal to:

SPIE, Boulder, CO

October 1992

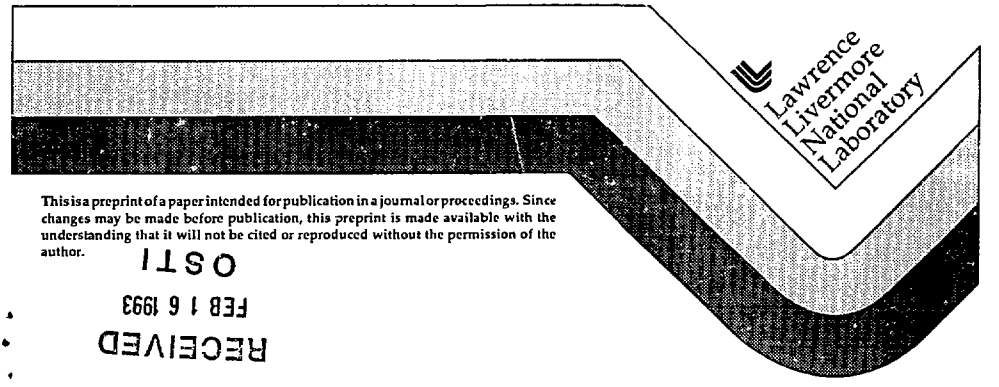

# Correlation of Damage Threshold and Surface Geometry of Nodular Defects in HR Coatings As Determined by In-Situ Atomic Force Microscopy

M.C. Staggs, M. R. Kozlowski, W.J. Siekhaus and M. Balooch
University of California
Lawrence Livermore Laboratory
P.O. Box 5508, L-490
Livermore, CA 94550

UCRL-JC--111464

DE93 007509

## ABSTRACT

Atomic force microscopy (AFM) was used to determine in-situ the correlation between the surface dimensions of defects in dielectric multilayer optical coatings and their susceptibility to damage by pulsed laser illumination. The primary surface defects studied were μm-scale domes associated with the classic nodule defect. The optical film studied was a highly reflective dielectric multilayer consisting of pairs of alternating $HfO_2$ and $SiO_2$ layers of quarter wave thickness at 1.06 μm. Nodule defect height and width dimensions were measured prior to laser illumination on two different samples. Correlation between these dimensions supported a simple model for the defect geometry. Defects with high nodule heights (> 0.6 μm) were found to be most susceptible to laser damage over a range of fluences between 0-35 J/cm$^2$ (1.06 μm, 10 ns, and $1/e^2$ diam. of 1.3 mm). Crater defects, formed by nodules ejected from the coating prior to illumination, were also studied. None of the crater defects damaged when illuminated over the same range of fluences that the nodule defects were subjected to.

## 1.INTRODUCTION:

It is well known that laser-induced damage in optical thin films often initiates at defects in the coatings.[1, 2] In many cases, these defects are the classic nodular defects formed due to shadowing effects initiated at seed particles during the deposition process.[1, 3] Laser interactions with these defects are important to the laser conditioning process used to increase the damage threshold of these coatings.[4] AFM studies have shown that the smoothing of nm-scale features on the coatings may be associated with the stabilization of these defects during laser conditioning.[4,5,6]

Not all defects that are illuminated are susceptible to laser-induced damage. Also the damage threshold of a coating often decreases as the density of defects increases. Both of these observations suggest that all defects are not the same. In a previous paper [2], we had used the AFM to identify three different types of defects in multilayer $HfO_2/SiO_2$ coatings. These types are the nodular defect observed as a shallow dome on the surface, a layered hole in which the nodule has been ejected revealing the coating layers, and a smooth hole in which the nodule has been ejected during the deposition process and subsequent layers had begun to fill it in. The purpose of the present paper was to determine which types and sizes of defects are most susceptible to laser damage. There are two main parts to this work: i) develop statistics on the heights and diameters of the defects in these coatings, and ii) determine any correlation between defect shape and damage threshold. In this study we will focus on the influence of 1064 nm radiation at 10 ns pulse lengths.

## 2. EXPERIMENTAL TECHNIQUES

Laser illumination was performed using our standard laser-damage testing systems. A 1064 nm neodymium YAG laser with a 10 ns pulsewidth and a beam diameter of 1.3 mm at $1/e^2$ was focused onto the sample surface using a lens with a focal length of 5 meters. Laser fluences were determined by beam profiling and total energy measurements.



* This work was performed under the auspices of the U.S. Department of Energy by Lawrence Livermore National Laboratory under Contract No. W-7405-ENG-48.

The AFM was incorporated into our laser-damage testing system for in-situ characterization of the optical surfaces. In these experiments, the sample is imaged with the AFM, illuminated with the laser, and then re-imaged. The ease with which this can be done has increased significantly over the last two years. Figure 1 shows the evolution of the AFM, resulting in vast improvements over prior in-situ AFM experiments.[7] For the last two years we have presented results obtained using a standard AFM system.[2,4] This system was limited to samples of approximately 1-cm diameter. The geometry of the experiment required large observation angles when locating coating defect sites with a low resolution (~ 65X) microscope. The sample was manually moved until a defect site was found. This was a very time consuming and tedious process. The defect was then imaged with the AFM, illuminated and then re-imaged with the AFM.

The present work began by incorporating the Stand Alone AFM[7] as part of the damage experiment. The Stand Alone feature allows us to image a surface of any size, including our standard 2-in. diameter samples. This system was then integrated into our Nomarski damage experiment, allowing the sample to be easily and quickly moved between the laser, the Nomarski (100X) microscope and the AFM. Defects were located with the Nomarski microscope. The sample was then rotated into a position that enabled imaging with the Stand Alone AFM. The sample was then further rotated into a position which allowed laser illumination. After illumination the defect was re-imaged with the AFM and the Nomarski microscope.

The latest stage of work was done using a Large Area AFM[7]. This system allowed rapid movement between the high resolution (~850X) optical microscope, the laser, and the AFM using a computer controlled x-y stage. Defects located using the optical microscope were easily moved under the AFM head and imaged via software controls. The sample was then positioned to a pre-determined coordinate allowing us to illuminate the defect site with laser pulses. Re-imaging of the defect was then performed in a matter of minutes. An equivalent amount of data which once took months with the standard AFM, weeks with the Stand Alone AFM, now can be expedited in a matter of a few days with the Large Area AFM.

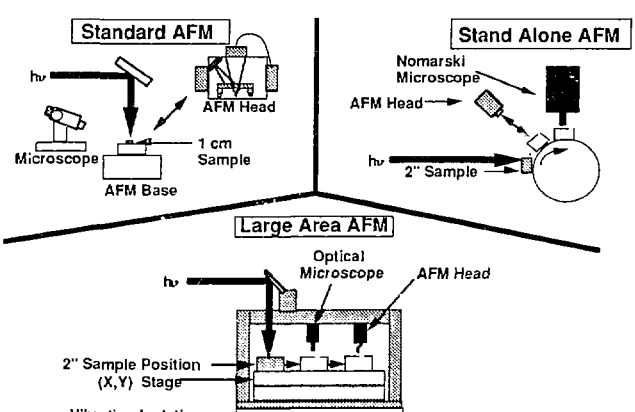


Fig. 1. Schematic representations of the AFM systems used for in-situ laser damage experiments.

## 3. GEOMETRIC MODEL OF NODULAR DEFECTS:

The seeds are assumed to be particles ejected from the source material during deposition. There are two principal mechanisms by which such particle ejection can occur: relief of temperature-induced stress and explosions caused by expansion of trapped gasses in the source material. Chow et al. [8] has recently shown that stress relief of temperature-induced phase transitions is the dominant cause of particle "spitting" in $HfO_2$. As a basis for interpreting the microscopy results, we propose a simple geometric model for nodular defects in multilayer coatings. The defects are assumed to be cylindrically symmetric with parabolic sides as shown in Fig. 2. This shape is characteristic of nodular defects formed on rotating substrates [3]. Based on our studies and the literature, we have assumed that the seeds initiating the nodule are spherical, are composed of coating material, and can be deposited at any time during the deposition process. We have also assumed that the deposition rate is the same at all angles so that the film thickness radially from the seed is the same as the vertical layer thickness on a perfect substrate. Therefore the resulting layers deposited above the seed are sections of concentric spheres. The intersection of these spheres with the undisturbed layer structure produces the parabolic shape of the defect observed in cross section. Based on these assumptions, the height of the nodule dome at the coating surface, h, is equal to the diameter of the defect seed, d.[9] The diameter of the nodule dome, D, is given by

$$D = (8\,d\,T)^{1/2}, \tag{1}$$

where T is the depth at which the seed is deposited. Consequently,

$$D = (8\,h\,T)^{1/2}. \tag{2}$$

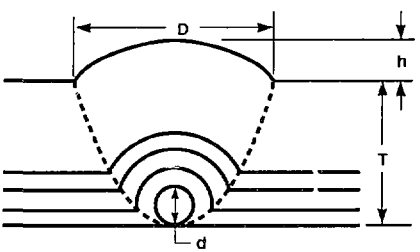


Fig. 2. Geometry of an ideal nodule defect in a multilater stack. The surface diameter, D, is given by Eqn. 2.

## 4. RESULTS AND DISCUSSION

The following results are from two $HfO_2/SiO_2$ HR coatings deposited under identical conditions but during two different coating runs. We will first discuss the results of the height-diameter study.

Sample 15D was first examined using the Stand Alone AFM. Defects to be studied were found by searching the surface with an optical microscope. The solid squares in Fig. 3 show the diameters and heights of 14 defects found over an area of a few square cm. The data show a general increase in defect diameter with height. In order to determine if our "random" selection of defects had somehow biased the data, we scanned an area of a few square millimeters with the Large Area AFM and imaged all defects found. Figure 3 shows

that this second set of data (open squares) perfectly overlaps the data from the Stand Alone AFM. The overlap of the data indicates that the correlation observed is significant over large areas of the sample. Figure 4 shows the data from Fig. 3 plotted as diameter squared versus height. The data forms a line that passes through the origin. This type of correlation is predicted from Eqn. 2 if all of the defects are initiated at the same depth, as would occur if the source became unstable and spit out particles only one time during the deposition. Solving for T from the data in Fig. 4 gives a seed depth of 3.5 μm. This is reasonable as the total coating thickness is about 4.3 μm.

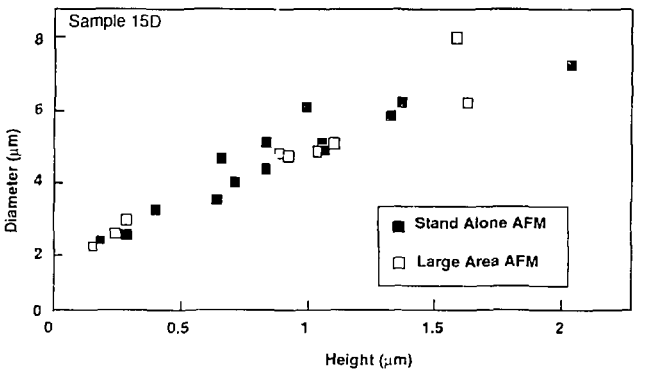


Fig. 3. Plot of diameter vs. height of nodular defects on sample 15D using the Stand Alone AFM and the Large Area AFM.

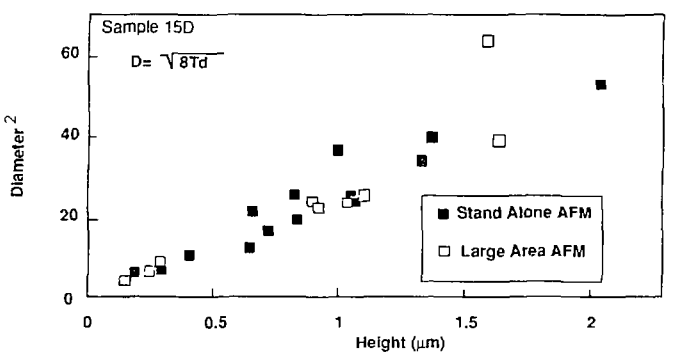


Fig. 4. Data from Fig. 3 (sample 15D)plotted as diameter squared vs. height.

Figure 5 is a diameter vs. height plot for another sample (09A) deposited in a different coating run. In this case the data points do not fall on a single curve. If the model of Eqn. 2 is correct, the data in Fig. 5 suggests that for this coating run the defects were initiated at a wide range of depths.

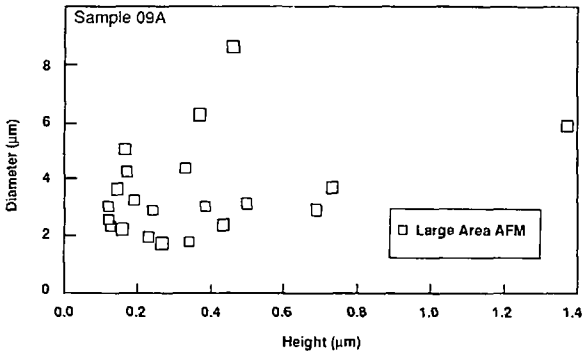


Fig. 5. Plot of diameter vs. height of nodular defects for sample 09A using the Large Area AFM system.

We next irradiated a large number of defects on these two samples at various laser fluences. Each defect was illuminated at only one fluence. The fluences ranged from 4 to 35 J/cm$^2$. The unconditioned (1-on-1) damage threshold for these coatings was near 4.7 J/cm$^2$. Figure 6 shows the heights of various defects on Sample 15D that were illuminated at the indicated fluences. The solid circles indicate defects that were damaged by the laser pulses. The data indicate that defects with heights above approximately 0.6 μm are most susceptible to damage. It is not clear from the data if the damage threshold varies with defect height or if there is only a threshold defect height above which damage always occurs (over the fluence range tested). Figure 7 shows a plot of illumination fluence versus defect diameter for the same set of defects. There is again a transition diameter, at about 4 μm, at which the defects have a high probability of damaging. The transition in Fig. 7 is expected since a transition was observed in the fluence-versus-height plot and there was a clear correlation between diameter and height for this sample.

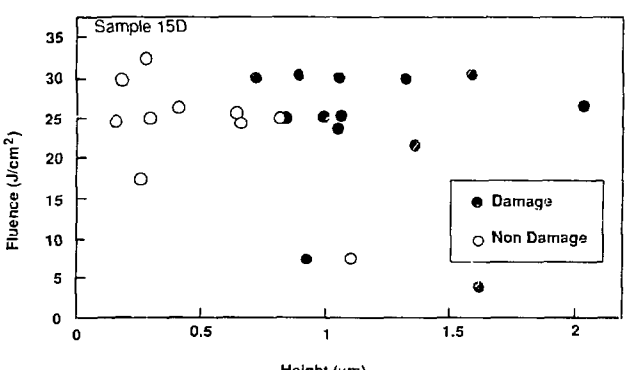


Fig. 6. Plot of fluence vs. height of nodular defects on sample 15D.

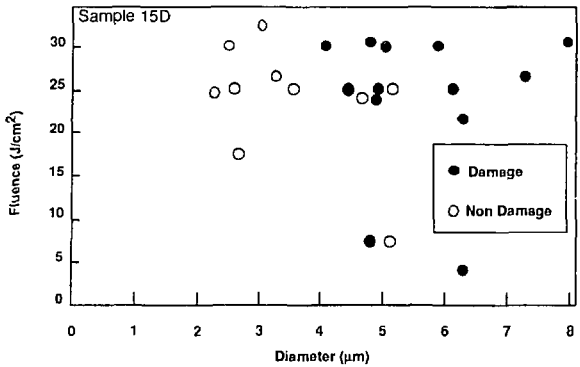


Fig. 7. Plot of fluence vs. defect diameter for the same set of defects shown in Fig. 6.

A similar set of illumination tests were performed on sample 09A. Figure 8 is the resulting plot showing the illumination fluence and height of the various defects tested. In this case we could find few defects with heights above 0.6 μm, but those we did illuminate always damaged. This set of data is therefore very consistent with the results shown in Fig. 6 for sample 15D. In the fluence-diameter plot for sample 09A (Fig. 9), however, no transition diameter is apparent. This is in contrast to the data for sample 15D where the damage susceptibility appeared to become high for defects with diameters above 4 μm. The data presented in Figs. 6 -9 therefore suggest that it is the defect height that most strongly determines a defects susceptibility to damage. We propose that the influence of damage susceptibility on defect diameter observed for sample 15D was only the result of the simple diameter-height correlation observed for that sample.

Finally, we illuminated approximately six crater defects (holes left by nodules ejected prior to illumination) that were found on the samples. Figure 10 shows that over the range of fluences where nodule defects were illuminated, none of the crater defects damaged. Nodule craters therefore do not appear to affect the damage threshold of these coating materials.

The mechanism explaining the increased damage susceptibility of the defects is not clear. One possible explanation is that the nodules increase the local electric fields in the coating. Bloembergen[10] has shown that simple defects such as cracks and voids produce such effects in bulk dielectric materials. DeFord and Kozlowski[11] have recently calculated the electric field enhancement due to ideal nodular defects in $HfO_2$/$SiO_2$ stacks. The calculations showed a general increase in E-field enhancement with increased defect seed diameter and, therefore, defect height. This agrees qualitatively with the data presented here. The trend observed in the modelling study was not monotonic, however, and no transition height was indicated. It is likely that the E-field enhancement at the defect explains only part of the overall laser damage process. The modelling results suggest that the E-field enhancement is more strongly influenced by the seed depth, T. In general, large shallow seeds showed the greatest E-field enhancement. No simple correlation between defect diameter and enhancement was indicated by the modeling results, in agreement with our experimental results. The modelling work also predicted that the crater defect would not increase the E-field magnitudes within the coating stack.[12] This result is consistent with our observation that the craters do not show an increased damage susceptibility.

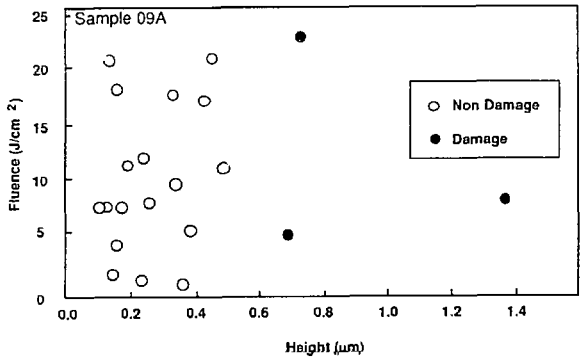


Fig. 8. Plot of fluence vs. height of various nodular defects found on sample 09A.

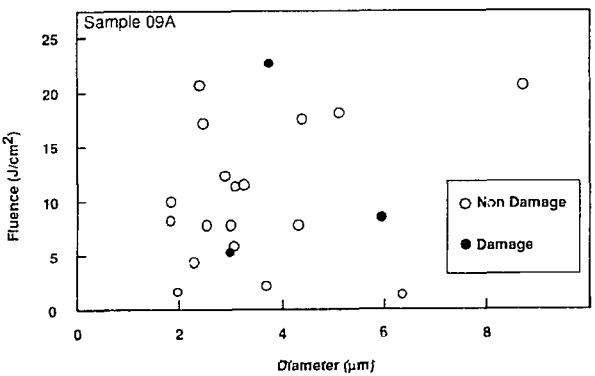


Fig. 9. Plot of fluence vs. diameter of the nodular defects found on sample 09A.

## 5. CONCLUSIONS.

Advances in Atomic Force Microscopy have made it easier to characterize and to monitor laser-induced damage at defects in optical coatings. In studies of $HfO_2/SiO_2$ multilayers we found that in some samples there is a strong correlation between the diameters and heights of nodular defects. Based on a simple model for the defect geometry, this result indicates that all seeds initiating defects on such samples may have been deposited at the same depth. On another sample, however, a correlation between the diameter and height of the defects was not observed, indicating that defects started at different depths during the deposition process. Laser illumination of these defects showed that defects with large heights (particularly those above 0.6 μm) are most susceptible to laser-induced damage. Nodule craters left by nodule ejected prior to illumination showed no increased damage susceptibility.

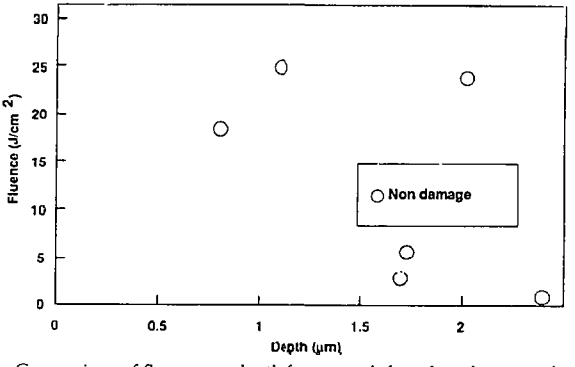


Fig. 10. Comparison of fluence vs. depth for crater defects found on samples 09A and 15D.

The qualitative increase in damage susceptibility with defect height and the lack of increased damage susceptibility of the crater defects can be explained using the results of E-field enhancement modelling studies on ideal nodular defects. A more complete understanding of the laser damage process would require consideration of mechanical and thermal processes as well. Also, the size of a defect which is most susceptible to laser damage is likely dependent on the wavelength and pulselength of the illumination.

## 6. ACHNOWLEDGEMENTS

Work performed under the auspices of the U.S. Department of Energy by Lawrence Livermore National Laboratories under contract No. W-7405-ENG-48.

## 7. REFERENCES:

[1] L. F. Johnson, E. J. Ashley, T. M. Donovan, J. B. Franck, R. W. Woolever, and R. Z. Dalbey, "Scanning electron microscopy studies of laser damage initiating defects in ZnSe/$ThF_4$ and SiH/$SiO_2$ multilayer coatings," *Laser Damage in Optical Materials: 1984*, NBS Special Pub. **727**, 1984, p. 356.

[2] M. R. Kozlowski, M. Staggs, M. Balooch, R. Tench, and W. Siekhaus, "The surface morphology of as-deposited and laser-damaged dielectric mirror coatings studied in-situ by Atomic Force Microscopy," *Scanning Microscopy Instrumentation:1991*, SPIE vol 1556, 1992.

[3] B. Liao, D. J. Smith, and B. McIntyre, "The formation and development of nodular defects in optical coatings," *Laser Induced Damage in Optical Materials: 1985*, NBS Special Publication **746**, 1985, p. 305.

[4] M. C. Staggs, M. Balooch, M. R. Kozlowski, and W. J. Siekhaus, "In Situ Atomic Force Microscopy of laser-conditioned and laser-damaged $HfO_2/SiO_2$ dielectric mirror coatings," *Laser-Induced Damage in Optical Materials:1991*, SPIE Vol. **1624**, 1992, p. 375.

[5] N.J. Hess, G.J. Exharos, and M. J. Iedema, "Atomic Force Microscopy of CW laser-conditioned and laser-damaged amorphous $TiO_2$ sol-gel films," *Laser-Induced Damage in Optical Materials: 1992*, SPIE, this proceedings vol., 1993.

[6] A.A.Tesar, M. Balooch, R. Tench, C. Stolz, T. Targinson and W. J. Siekhaus, "Examination of laser conditioning using the Atomic Force Microscope," *Laser Induced Damage in Optical Materials: 1991*, SPIE Vol. 1624, 398, 1992.

[7] All AFMs are products of Digital Instruments Inc, Santa Barbara, CA 93117
[8] R. Chow, S. Falabella, G.E. Loomis, F. Rainer, C.J. Stolz and M.R. Kozlowski,"Reactive evaporation of low defect density hafnia," *Laser-Induced Damage in Optical Materials: 1992*, SPIE, this proceedings vol., 1993.
[9] K. H. Guenther, "Microstructure of vapor-deposited optical coatings," *Applied Optics*, **23**, 1984, p. 3806
[10] N. Bloembergen, "Role of cracks, pores, and absorbing inclusions on laser induced damage thresholds at surfaces of transparent dielectrics," *Applied Optics*, **12** , 1973, p. 661.
[11] J. DeFord and M. R. Kozlowski, "Modelling of electric field enhancements at nodular defects in dielectric multilayer coatings,"*Laser-Induced Damage in Optical Materials: 1992*, SPIE, this proceedings vol., 1993.
[12] J. DeFord and M. R. Kozlowski, unpublished results, Lawrence Livermore National Laboratory, 1992.